Pergamon

The effect of fluoride on the dissolution rates of natural glasses at pH 4 and 25°C

Domenik Wolff-Boenisch,[1,*,†] Sigurdur R. Gislason,[1] and Eric H. Oelkers[2]

[1]Science Institute, University of Iceland, Dunhagi 3, 107 Reykjavik, Iceland
[2]Géochimie: Transferts et Mécanismes, CNRS/UMR 5563–Université Paul Sabatier, 38 rue des Trente-six Ponts, 31400 Toulouse, France

Abstract—Far-from-equilibrium, steady-state dissolution rates at pH 4 of a suite of natural glasses, ranging from basaltic to rhyolitic in composition, have been determined as a function of aqueous fluoride concentrations up to 1.8×10^{-4} mol/kg in mixed-flow reactors. Dissolution rates of each of these glasses increase monotonically with increasing aqueous fluoride concentration. Measured dissolution rates are found to be consistent with both the Furrer and Stumm (1986) surface coordination model and the Oelkers (2001) multi-oxide dissolution model. Application of the latter model yields the following equation that can describe all measured rates as a function of both glass and aqueous solution composition:

$$\log (r_{+,geo}/(mol/m^2/s)) = [-0.086 \cdot SiO_2(wt\%) - 2.23] + [-0.0067 \cdot SiO_2(wt\%) + 0.683] \cdot \log (a_{H^+}^3/a_{Al^{3+}})$$

where $r_{+,geo}$ represents the far-from-equilibrium dissolution rate, normalized to geometric surface area, $SiO_2(wt.\%)$ refers to weight percent of SiO_2 in the glass, and a_i denotes the activity of the subscripted aqueous species. Computed glass dissolution rates increase with increasing aqueous fluoride concentration due to the formation of aqueous Al-fluoride complexes, which decrease $a_{Al^{3+}}$. This rate expression can be used to predict far-from-equilibrium dissolution rates of natural glasses in a variety of natural environments. Comparison of rate predictions with the composition of natural fluids suggests that the presence of aqueous fluoride can enhance natural glass dissolution rates by an order of magnitude or more in a variety of geochemical systems. *Copyright © 2004 Elsevier Ltd*

1. INTRODUCTION

The overall goal of this study is the improved understanding of the dissolution rates of natural glasses as a function of both their composition and aqueous solution composition. Towards this goal the dissolution rates of 7 natural glasses of distinct composition have been measured at 25°C and pH 4 as a function of total aqueous fluoride concentration. The interpretation of these results through transition state theory leads to a general equation describing far-from-equilibrium natural glass dissolution rates. The purpose of this manuscript is to report the results of this combined experimental and theoretical study.

Owing to its abundance and rapid mechanical and chemical weathering, volcanic glass is of major importance in the global and local cycling of numerous elements and chemical species at the Earth's surface. The chemical weathering of volcanic glasses in soils governs the soil fertility and the formation of clay minerals (e.g., Shoji et al., 1993; Nieuwenhuyse et al., 2000; Arnalds and Kimble, 2001; Stefansson and Gislason, 2001; Vacca et al., 2003). For example, the high volcanic activity on the islands and mountains spanning the Pacific 'Ring of Fire' produces considerable glassy material like ash, pumice, and scoria. Its subsequent weathering generates and-isols, a very fertile soil that supports a dense vegetation cover in moist climates, including Hawaii, Chile, Indonesia, and South Japan. Environmental conditions including temperature, rainfall and vegetation strongly influence the rate of weathering

(Supriyo et al., 1992; Dahlgren et al., 1993; Brady and Carroll, 1994; Gislason et al., 1996; Dubroeucq et al., 1998; Moulton et al., 2000; Chadwick et al., 2003).

Natural solutions such as those found in soils often contain complex-forming ligands, many of which have been found to influence dissolution rates at acid conditions. Such ligand-promoted dissolution has frequently been attributed to the capacity of these organic ligands to form surface complexes, (e.g., Huang and Kiang, 1972; Wieland et al., 1988; Stumm, 1997; Drever and Stillings, 1997; Ullman and Welch, 2002 and references cited therein). Ernsberger (1959) and Bacon and Raggon (1959) attributed the dissolution promoting effect of organic ligands and chelates on synthetic glasses to an increase in the Si-solubility. For the case of natural glasses, Oelkers and Gislason (2001) observed increased basaltic glass dissolution rates with increasing aqueous oxalate concentration. They ascribe this effect to the aqueous complexation of oxalate with aluminium diminishing thus the dissolution rate inhibitory effect of aqueous Al^{3+}.

Building upon these previous studies, the present study is focussed on the effect of aqueous fluoride on natural glass dissolution rates. The aggressive nature of fluoride towards Al bearing layer-silicates and oxides was described nearly 40 yr ago (Huang and Jackson, 1965). Grandstaff (1977) reported an increase in dissolution rates of bronzite orthopyroxene in the presence of aqueous fluoride; a similar effect was observed for clay minerals (Gajam and Raghavan, 1985; Arocena et al., 1995; Luther et al., 1996). The dissolution rates of feldspars have been reported to increase notably with increasing aqueous fluoride concentration (Amrhein and Suarez, 1988; Shotyk and Nesbitt, 1992; Harouiya and Oelkers, 2004). An increase in the dissolution rates of aluminium oxide and (oxy)hydroxides in

---

* Author to whom correspondence should be addressed (dwolff-boenisch@ucmerced.edu).
† *Present address:* Sierra Nevada Research Institute, University of California, P.O. Box 2039, Merced, CA 95344.

the presence of aqueous fluoride was observed by Zŭtić and Stumm (1984), Kraemer et al. (1998), and Nordin et al. (1998, 1999). Steel et al. (2001) reported the preferential dissolution of aluminosilicates in the presence of HF. Other studies have noted the strong formation of aqueous aluminium fluoride complexes (e.g., Plankey et al., 1986; Tagirov et al., 2002). Driscoll et al. (1980) stated that aluminium-fluoride complexes are the dominant inorganic aluminium species in many natural waters. These studies demonstrate that the presence of aqueous fluoride not only significantly enhances aluminosilicate dissolution rates but also the solubility of these minerals (cf. Elrashidi and Lindsay, 1987). All of these studies illustrate the relevance of aqueous fluoride in water-aluminosilicate interaction in natural processes. To further improve our understanding of such processes, this study presents for the first time measured dissolution rates of a suite of distinct natural glasses as a function of aqueous fluoride concentration.

2. THEORETICAL BACKGROUND

The standard state adopted in this study is that of unit activity for pure minerals and H_2O at any temperature and pressure. For aqueous species other than H_2O, the standard state is unit activity of the species in a hypothetical 1 molal solution referenced to infinite dilution at any temperature and pressure. All aqueous activities in the present study were generated using PHREEQC 2.6 computer code (Parkhurst and Appelo, 1999). Equilibrium constants were taken from the PHREEQC database for all species and minerals other than aqueous Al-bearing complexes, which were taken from Tagirov and Schott (2001). The significant Al-bearing aqueous species considered in the thermodynamic model are Al^{3+}, AlF^{2+}, AlF_2^+, AlF_3^0, AlF_4^-, $Al(OH)^{2+}$, $Al(OH)_2^+$, and $Al(OH)_2F^0$.

The overall glass dissolution rate may be influenced by numerous factors including 1) the aqueous transport of chemical species away from its surface (cf. Murphy et al., 1989); 2) the effect of reverse reaction at near to equilibrium conditions (cf. Grambow, 1985; Oelkers et al., 1994); and 3) the far-from-equilibrium dissolution rate. The goal of the current study is to compare the far-from-equilibrium dissolution rates of natural glasses as a function of the total aqueous fluoride concentration. Experimental conditions were chosen, therefore, to assure that all rates measured in the present study are surface reaction controlled and at far-from-equilibrium conditions.

The variation in the far-from-equilibrium surface area normalized forward dissolution rate with aqueous solution composition can be deduced from the dissolution mechanism. Natural glass dissolution rates measured in the present study are interpreted in accord with the basaltic glass dissolution mechanism proposed by Oelkers and Gislason (2001). Within this mechanism, basaltic glass dissolution is assumed to consist of a series of metal for proton exchange reactions at the glass surface. The equilibrium constants of exchange reactions involving monovalent and divalent interstitial cations, which are commonly viewed as being loosely bound to the glass structure (e.g., Berger et al., 1987; Crovisier et al., 1987; Guy and Schott, 1989; Petit et al., 1990), are sufficiently large such that these metals are essentially completely removed from the basaltic glass near surface. These metals have also been observed to be preferentially removed from the near surface of more silica rich

glasses (Taniguchi, 1980; White and Claassen, 1980; White, 1983; Allnatt et al., 1983; Fiore et al., 1999). In contrast, equilibrium constants for those exchange reactions involving trivalent cations, which are generally viewed as being strongly bound, are relatively small such that only a small fraction of these cations are removed via proton exchange reactions. The final and rate limiting step of basaltic glass dissolution is the liberation of partially detached Si tetrahedra from the basaltic glass surface. These partially detached Si are those that are bound to the glass structure by only two bridging oxygens and can be formed by the removal of adjoining trivalent cations. Within the formalism of transition state theory, basaltic glass dissolution rates are, therefore, proportional to the concentration of these partially liberated Si tetrahedra. Taking account of the law of mass action of the Al for proton exchange reaction that creates partially liberated Si at the basaltic glass surface, Oelkers (2001), Oelkers and Gislason (2001), and Gislason and Oelkers (2003) proposed the following equation to describe far-from-equilibrium surface reaction controlled basaltic glass dissolution rates at constant temperature:

$$r_+ = k \left(\frac{a_{H^+}^3}{a_{Al^{3+}}} \right)^n \tag{1}$$

where r_+ represents the forward dissolution rate, k denotes a rate constant, a_i designates the aqueous activity of the subscripted species, and n stands for a stoichiometric constant equal to the reciprocal of the number of partially detached Si tetrahedra formed from each Al for proton exchange reaction. Oelkers and Gislason (2001) reported that for the case of basaltic glass 3 partially detached Si tetrahedra form from each Al for proton exchange reaction and thus $n = [1/3]$. Eqn. 1 was shown to successfully describe basaltic glass dissolution rates as a function of pH and the concentration of aqueous Al, Si, and organic acids. The logarithmic analog of Eqn. 1 is given by:

$$\log r_+ = \log k + n \cdot \log(a_{H^+}^3 / a_{Al^{3+}}) \tag{2}$$

If the reaction mechanism of the natural glasses investigated in this study at pH 4 and 25°C is similar to that of basaltic glass, $\log r_+$ should be a linear function of $\log (a_{H^+}^3 / a_{Al^{3+}})$.

The present study is focussed on the effect of aqueous fluoride on natural glass dissolution. The effect of aqueous fluoride on dissolution rates is taken into account in Eqn. (1) and (2) through its effect on aqueous aluminium activity. Aqueous aluminium activity decreases at acid conditions with increasing fluoride concentration through the formation of aqueous aluminium-fluoride complexes. Figure 1 depicts the logarithm of aqueous aluminium bearing species activities computed as a function of the logarithm of total fluoride solution concentration in pH 4 solutions and a temperature of 25°C. This figure was generated using PHREEQC 2.6 assuming a total fixed Al concentration of 10^{-6} mol/kg. At very low total fluoride concentrations the predominant species is Al^{3+} but with increasing fluoride concentrations the predominance is taken over successively by AlF^{2+}, AlF_2^+, AlF_3, and ultimately AlF_4. The formation of aqueous aluminium fluoride complexes leads to a strong decrease in aqueous Al^{3+} activity from 10^{-6} in F-free solutions to 10^{-21} in solutions containing 0.1 mol/kg
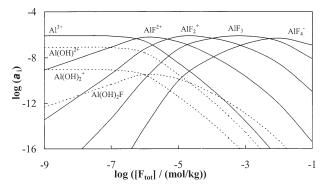
Fig. 1. Computed activities of aqueous Al^{3+}, AlF^{2+}, AlF_2^+, AlF_3^0, AlF_4^-, $Al(OH)^{2+}$, $Al(OH)_2^+$, and $Al(OH)_2F^0$ as a function of the total aqueous F concentration at pH 4 and 25°C. The curves were generated with PHREEQC 2.6 and for a solution having a total aluminium concentration of 10^{-6} mol/kg.

total fluoride. The decrease in aqueous aluminium activity leads directly to increased dissolution rates in Eqns. (1) and (2).

3. EXPERIMENTAL METHODS

A thorough description of the glass specimens and the experimental methods used in the present study is provided in Wolff-Boenisch et al. (2004). Six of the glass samples used in this study originated from Icelandic volcanic eruptions; one specimen stems from an ignimbrite pyroclastic flow from California. The volcanic glasses were dried, subsequently cleaned with a stiff-bristled brush and shaken to remove adhered particles. All samples were ground in plastic bags using a plastic hammer in an attempt to induce minimum strain to the fresh surfaces. The 45–125 μm size fraction was then ultrasonically cleaned in cycles of deionized water and acetone, separating and discarding the ultra fine suspension at the end of each cleaning cycle. Table 1 provides the chemical analyses of the specimens.

All dissolution experiments were conducted in titanium mixed flow-through reactors at 25°C, pH 4 and constant ionic strength of 10 mM. Inlet solutions were comprised of Millipore™ water, and Merck analytical grade NH_4Cl, HCl, and HF. The outlet solution was filtered through a 0.2 μm cellulose acetate membrane filter, acidified with concentrated supra-pure HNO_3 and analysed for the silica content. Each experiment was run until steady-state was attained. Steady-state in the mixed flow reactor experiments is assumed when the silica outlet concentration remains constant for an amount of time exceeding 10 times the residence time of the reactor. The residence time of the experiments performed in the present study is between 2 and 6 h.

All dissolution rate experiments were performed as an experimental series on individual glass powders. The initial inlet solution was fluoride-free. Once the first steady-state was reached in this fluoride-free inlet solution a new F-bearing inlet solution was passed through the reactor, first in the lowest concentration (30 μmol/kg). Then, after each steady-state, the fluoride concentration of the inlet solution was increased from 60 μmol/kg to 90 μmol/kg and then to 180 μmol/kg.

Multi-element analyses were performed by ICP-AES to determine outlet solution concentrations of Si, Al, Na, Mg, Ca, and Fe in all solutions. Species distribution calculations with PHREEQC 2.6 indicate that all pH 4 outlet solutions were undersaturated with respect to all potential secondary phases.

4. RESULTS AND DISCUSSION

All experimental conditions were run until steady-state outlet solutions were attained. Steady-state in each experiment was assumed once the outlet solution Si concentration remained constant, within analytical uncertainty, over a period of at least 10 residence times. Representative examples of the approach to steady-state during the experimental series can be seen in Figure 2. For each set of experimental conditions, outlet solution Si concentration increases smoothly until the steady-state Si concentration was attained (Fig. 2a). Each steady-state plateau corresponds to a distinct fluoride concentration increasing from left to right (0, 30, 60, 90, 180 μmol/kg). The release of other elements exhibits somewhat different behaviours than that of Si, as can be seen in Figures 2b and c. Al is released preferentially compared with Si at the onset of each experimental series. The outlet solution Al/Si ratio attains a stoichiometric proportion only after ~0.5% of the natural glass is dissolved. A similar behaviour is commonly observed for the relative release of Fe, Ca, Mg, and Na, although in some instances Ca, Mg and/or Na did not attain stoichiometric release rates before the end of the experimental series. For example, the results shown in Figure 2c illustrate the release rates relative to Si of Al, Fe, Ca, Mg, and Na during the dissolution of the rhyolite BT. All of these metals are released preferentially compared to Si at the onset of the experimental series; all but Mg approach stoichiometric release rates relative to Si after ~0.5% of the glass was dissolved. The preferential release of Al and other elements from the glass surface at the beginning of these experiments is consistent with the multi-oxide dissolution mechanism described above, which is initiated by the exchange of these cations with protons at the glass surface followed by the rate limiting detachment of Si.
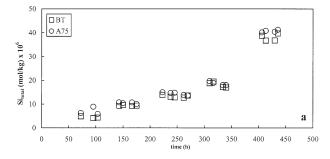
Far-from-equilibrium steady-state geometric specific surface area normalized dissolution rates $r_{+,geo}$ are calculated using:
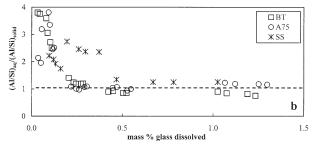
$$r_{+,geo} = \frac{C_{Si} \cdot fr}{A_{geo} \cdot m} \qquad (3)$$

where C_{Si} designates the aqueous Si concentration of the outlet solution (mol/kg), fr represents the fluid flow rate (kg/s), A_{geo} is the initial geometric surface area of the dissolving glass (m^2/g), and m the mass of sample (g). The geometric specific

Table 1. XRF chemical analyses of the volcanic glasses in weight percent. Major element reproducibility yielded relative standard deviations <2% for all the oxides.

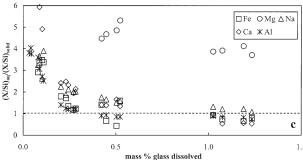| Name	SiO_2	TiO_2	Al_2O_3	Fe_2O_3	FeO	MnO	MgO	CaO	Na_2O	K_2O	P_2O_5	LOI
BT	72.62	0.08	12.48	0.78	0.11	0.03	0.09	0.48	3.79	4.38	0.01	4.83
Ö62	70.64	0.24	13.00	2.40	1.18	0.1	0.02	0.97	5.45	3.41	0.02	1.95
H3W	69.79	0.21	13.79	1.15	2.32	0.11	0.11	2.08	4.83	2.48	0.04	1.90
A75	69.28	0.90	12.42	2.48	2.09	0.1	0.97	2.81	3.74	2.21	0.19	1.70
HZ0	62.80	0.96	15.34	2.64	4.53	0.17	1.4	4.57	4.35	1.55	0.34	0.20
SLN	62.76	1.26	14.36	2.09	4.15	0.19	1.05	2.94	4.62	2.55	0.3	2.64
SS	46.48	2.46	16.35	2.57	9.66	0.19	5.88	9.87	3.6	0.67	0.33	−0.13

Fig. 2. Representative examples of the temporal evolution of metal release rates: a) outlet Si concentrations during experimental series BT and A75 as a function of elapsed time. Each of the five individual data clusters represents a steady-state corresponding to distinct aqueous fluoride concentrations of 0, 30, 60, 90, 180 μmol/kg from left to right in the figure; b) variation of the ratio of the relative release rate of Al versus Si as a function of the mass percent glass dissolved during experimental series of BT (rhyolite), A75 (rhyolite), and SS (basalt); c) variation of the ratio of the relative release rate of Al, Fe, Ca, Mg and Na versus Si as a function of the percent glass dissolved during experimental series BT.

surface area A_{geo} used in Eqn. (3) to compute rates is assumed to be constant in each experiment and is calculated using (Brantley et al., 1999; Gautier et al., 2001):

$$A_{geo} = \frac{6}{\rho \cdot d_{eff}} \qquad (4)$$

where ρ is the glass density and d_{eff} is the effective particle diameter. The number 6 is based on the assumption that grains have a regular and smooth spherical shape. Assuming a homogeneous particle distribution, d_{eff} can be obtained from (Tester et al., 1994):

$$d_{eff} = \frac{d_{max} - d_{min}}{\ln\left(\dfrac{d_{max}}{d_{min}}\right)} \qquad (5)$$

where d_{max} and d_{min} refer to the maximum and minimum particle size of the size fraction used in the experiments. The ratio between BET and geometric surface area (A_{BET}/A_{geo}) is the roughness factor (Jaycock and Parfitt, 1981). The surface areas, roughness factors and calculated glass densities (ρ) of all glass powders used in the present study are listed in Table 2. Rates have been normalized with respect to geometric rather than BET surface areas because these have been observed to be more consistent with natural glass dissolution behaviour (Wolff-Boenisch et al., 2004). The reasons that geometric surface areas are believed to be more consistent with the dissolution behaviour of natural glass include 1) BET surface area measurements are influenced by the potential presence of non-reactive phases such as iron oxides; 2) BET surface area measurements may be influenced by the presence of less reactive internal surfaces (cf. Anbeek 1992a, 1992b, 1993); and 3) BET surface areas can change significantly during dissolution experiments (e.g., Brantley and Chen, 1995) which make application of such surface areas ambiguous. Moreover, Wolff-Boenisch et al. (2004) found that correlations between glass Si content and geometric surface area normalized dissolution rates were stronger than those found with their BET surface area normalized counterparts. All experimentally determined steady-state dissolution rates are listed in Table 3. Uncertainties associated with the rate constants arise from a variety of sources, including the measurement of aqueous solution concentrations, fluid flow rates, and the determination of the specific glass surface areas. An overall uncertainty of the geometric surface area normalized dissolution rates ($r_{+,geo}$) generated in this study are estimated to be ±0.3 log units (cf. Wolff-Boenisch et al., 2004).

All dissolution rates measured in the present study are illustrated in Figure 3 as a function of aqueous fluoride concentra-

Table 2. Summary of physical properties of the glass powders used in this study.

Sample	Volcanic Name	Glass Density* g/cm^3	A_{BET} cm^2/g/10^4	A_{geo} cm^2/g	Roughness Factor
BT	rhyolite	2.31	3.12	332	94
Ö62	rhyolite	2.36	0.43	324	13
H3W	rhyolite	2.42	1.08	316	34
A75	rhyolite	2.45	1.41	312	45
HZ0	dacite	2.59	0.62	296	21
SLN	dacite	2.55	2.65	301	88
SS	basalt	3.00	0.19	255	8

* Corresponds to the particle density.

Table 3. Experimental results of the dissolution rate experiments. The seven glasses are ordered from high to low silica content. The capital letter F in the glasses' names denotes the experimental fluoride series (cf. Wolff-Boenisch et al., 2004).

Sample	Temp. °C	Mass[£] g	pH*	Flow Rate g/min	Si_{total} $\mu mol/kg$	Al_{total} $\mu mol/kg$	Al/Si[#]	Log $(a_H^3/a_{Al^{3+}})$	Log $r_{+,geo}$ mol/m²/s	F_{tot} $\mu mol/kg$
BTF-3	25	7.00	4.11	0.83	4.34	3.30	3.8	−6.5	−9.56	0
BTF-5	25	7.00	4.09	0.97	9.60	5.95	3.1	−3.9	−9.18	30
BTF-8	25	7.00	4.04	1.37	13.92	3.95	1.4	−2.6	−8.87	60
BTF-14	25	7.00	3.92	1.79	19.50	3.66	0.9	−1.8	−8.60	90
BTF-19	25	7.00	3.84	1.84	36.77	6.08	0.8	−1.1	−8.31	180
Ö62F-4	25	8.01	4.11	0.93	2.34	2.32	4.6	−6.3	−9.85	0
Ö62F-7	25	8.01	4.14	1.33	10.19	1.80	0.8	−2.5	−9.06	60
Ö62F-10	25	8.01	4.08	1.61	13.95	1.26	0.4	−1.7	−8.84	90
H3WF-1	25	4.80	4.03	0.87	2.91	3.19	4.7	−6.2	−9.55	0
H3WF-5	25	4.80	4.08	0.95	9.85	5.03	2.2	−3.7	−8.99	30
H3WF-8	25	4.80	4.04	1.37	13.07	2.81	0.9	−2.5	−8.71	60
H3WF-14	25	4.80	3.92	1.89	16.12	1.85	0.5	−1.5	−8.48	90
H3WF-19	25	4.80	3.81	2.04	31.20	2.01	0.3	−0.5	−8.16	180
A75F-1	25	7.61	4.15	0.87	6.23	2.81	2.1	−6.5	−9.43	0
A75F-5	25	7.61	4.19	0.96	10.40	7.36	3.4	−4.4	−9.15	30
A75F-10	25	7.61	4.10	1.38	14.82	3.04	1.0	−2.7	−8.84	60
A75F-14	25	7.61	4.01	1.90	18.95	4.27	1.1	−2.2	−8.59	90
A75F-20	25	7.61	3.90	2.06	41.21	10.06	1.2	−1.5	−8.22	180
HZ0F-1	25	5.53	4.04	0.97	2.68	2.19	2.8	−6.1	−9.53	0
HZ0F-5	25	5.53	4.02	1.20	11.19	3.24	1.0	−3.2	−8.87	30
HZ0F-8	25	5.53	4.00	1.57	15.34	3.31	0.7	−2.4	−8.61	60
HZ0F-10	25	5.53	4.04	1.85	17.21	2.63	0.5	−2.0	−8.49	90
HZ0F-15	25	5.53	3.96	2.68	28.96	1.97	0.2	−0.8	−8.10	180
SLNF-3	25	5.02	4.12	1.26	6.61	6.71	3.8	−6.8	−9.04	0
SLNF-6	25	5.02	4.24	1.26	15.37	13.66	3.3	−5.4	−8.67	30
SLNF-9	25	5.02	4.17	1.65	17.90	11.26	2.3	−3.8	−8.49	60
SLNF-10	25	5.02	4.12	1.87	18.70	9.85	2.0	−3.0	−8.41	90
SLNF-13	25	5.02	3.94	2.68	31.20	3.41	0.4	−1.1	−8.03	180
SSF-4	25	2.50	4.17	0.98	5.87	4.25	1.7	−6.7	−8.82	0
SSF-5	25	2.50	4.75	1.04	13.27	15.05	2.7	−5.8	−8.45	60
SSF-12	25	2.50	4.56	1.71	26.91	13.97	1.3	−4.6	−7.92	90

[£] Mass prior to dissolution experiment.
* Measured at 25°C.
# molar (Al/Si)aq/(Al/Si)glass ratio.

tion. Seven natural glasses (4 rhyolites, 2 dacites, 1 basalt) with distinct Si contents were studied. At zero total fluoride concentration, $r_{+,geo}$ is highest for the basaltic glass and decreases with increasing glass silica content. This relationship has been observed in many glass studies and is consistent with the concept that the higher the silica polymerisation of the glass the more resistant it is to dissolution; this relationship is discussed in detail in Wolff-Boenisch et al. (2004). Measured glass dissolution rates increase substantially with increasing aqueous fluoride concentration, and the trend of decreasing rates with increasing glass silica content is respected at all of the aqueous fluoride concentrations considered in this study. It is also apparent in Figure 3 that the effect of aqueous fluoride on basaltic glass dissolution rates is stronger than that of the more Si-rich glasses.

4.1. Variation of Rates with $(a_H^3/a_{Al^{3+}})$ and Consistency with the Multi-Oxide Dissolution Model

The degree to which measured rates are consistent with Eqn. 1 and the dissolution mechanism proposed by Oelkers (2001), Oelkers and Gislason (2001), and Gislason and Oelkers (2003) can be assessed by considering the variation of measured $r_{+,geo}$ with

$(a_H^3/a_{Al^{3+}})$. This relationship is shown in Figure 4. Within uncertainty, $r_{+,geo}$ is a linear function of log $(a_H^3/a_{Al^{3+}})$. This observation is consistent with the possibility that the dissolution rates of the natural glasses considered in the present study are controlled by the liberation of partially detached Si tetrahedra and that they are formed through proton/aluminium exchange reactions. Note however, the slope of these curves differ from [1/3], which is the slope found for basaltic glass (Oelkers and Gislason, 2001; Gislason and Oelkers, 2003). Rather, n apparently depends on the glass chemical composition. This variation is displayed in Figure 5 where n is plotted against the glass silica content. One glass, SLN, exhibits an n that is very small compared to the other glasses (see Fig. 4f). However, n of the remaining six glasses plus that reported for basaltic glasses by Gislason and Oelkers (2003) can be satisfactorily approximated by a linear least square fit. To maintain internal consistency, the literature value was not included in the linear regression analysis, but it is evident that it is consistent with the results of the present study. The equation for the regression line is:

$$n = -0.0067 \cdot SiO_2(wt\%) + 0.683 \qquad (6)$$
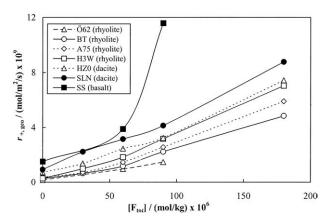
where SiO_2(wt.%) designates weight percent of SiO_2 in the

Fig. 3. Far-from-equilibrium dissolution rates ($r_{+,geo}$) of the natural glasses as a function of total F concentration in the solution ($[F_{tot}]$). Each data point represents a steady-state rate at a total F concentration of 0, 30, 60, 90, or 180 μmol/kg. The dashed and solid lines illustrate the general trend of each glass.

glass. The increase of n with decreasing glass silica content is itself consistent with the corresponding increasing non-linearity of the dissolution rate versus aqueous fluoride curves content shown in Figure 3. A similar least square fit can be generated of the log k values (Eqns. 1, 2), as shown in Figure 6, which yields:

$$\log (k/(mol/m^2/s)) = -0.086 \cdot SiO_2(wt\%) - 2.23 \quad (7)$$

Substituting Eqn. (6) and (7) into Eqn. (2) leads to the following expression describing the far-from-equilibrium glass dissolution rates as a function of their silica content at 25°C:

$$\log (r_{+,geo}/(mol/m^2/s)) = [-0.086 \cdot SiO_2(wt\%) - 2.23]$$
$$+ [-0.0067 \cdot SiO_2(wt\%) + 0.683] \cdot \log (a_{H^+}^3/a_{Al^{3+}}) \quad (8)$$

The degree to which Eqn. 8 can describe measured dissolution rates can be assessed with the aid of Figure 7. It can be seen that 38 of the 48 measured $r_{+,geo}$ are reproduced within an uncertainty of 0.3 log units; the average difference between measured and calculated rates is 0.2 log units. The results described above illustrate that experimentally measured glass dissolution rates are consistent with the Oelkers (2001) multi-oxide dissolution model, where natural glass dissolution consists of a series of metal-proton exchange reactions at the glass surface followed by the breaking of partially detached tetrahedrally coordinated Si atoms. The observation that the parameter n varies systematically with glass Si content suggests that the number of partially detached Si atoms created from the removal of each Al atom via Al-proton exchange reactions depends on glass composition. The rates measured in the present study show that the parameter n decreases with the SiO_2 content of the glass. Within the Oelkers (2001) multi-oxide dissolution model, this implies that the number of partially detached Si atoms on the glass surface created by the removal of each Al atom increases with decreasing glass SiO_2 content. The increasing value of k with decreasing SiO_2 content may also reflect an increase in the number of partially detached Si on the glass surface with decreasing SiO_2 content.

4.2. Surface Coordination Models

A different approach to describing the variation of dissolution rates with aqueous solution composition is based on a surface coordination model. Furrer and Stumm (1986) found that at acid conditions and in the absence of complex-forming ligands the dissolution rates of δ-Al_2O_3 can be considered to be proportional to the concentration of surface attached protons per unit area $\{H^+\}$. In the presence of ligands the proton-promoted ($r_{+,geo,H}$) and ligand-promoted ($r_{+,geo,L}$) dissolution occur simultaneously without affecting each other. Rates within this surface coordination model can be described using:

$$r_{+,geo} = r_{+,geo,H} + r_{+,geo,L} = k_H\{H^+\}^h + k_L\{L^-\}^l \quad (9)$$

where k_H and k_L are rate constants and h and l reaction orders, respectively. This equation was successfully applied in a modified form by Amrhein and Suarez (1988) to describe the ligand-promoted dissolution rates of anorthite. Eqn. 9 can be arranged to give:

$$r_{+,geo} - r_{+,geo,H} = r_{+,geo,L} = k_L\{L^-\}^l \quad (10)$$

The logarithmic analog of Eqn. 10 is

$$\log (r_{+,geo} - r_{+,geo,H}) = \log k_L + l \cdot \log \{L^-\} \quad (11)$$

It follows that within the surface coordination model log ($r_{+,geo}$ − $r_{+,geo,H}$) should be a linear function of log $\{L^-\}$; the slope of this line represents l and the y-intercept yields log k_L. Although the ligand concentration on the surface $\{L^-\}$ is unknown it is often assumed to be proportional to the aqueous ligand activity, in this study the fluoride activity (a_{F^-}). In the present study, $r_{+,geo,H}$ corresponds to measured $r_{+,geo}$ in F-free aqueous solutions. The degree to which this surface coordination model is consistent with the experimental results obtained can be gauged with the aid of Figure 8. Only five glasses are considered in this figure because the remaining glasses SS and Ö62 were dissolved at only two total fluoride concentrations; two data points could only yield a straight line in Figure 8. Four of the five glasses plotted in Figure 8 lie on a straight line consistent with the surface coordination model. The slopes are close to one suggesting a first order reaction of the ligand promoted dissolution $r_{+,geo,L}$ with respect to a_{F^-} for all these glasses. This same reaction order was determined by Furrer and Stumm (1986) for δ-Al_2O_3 and BeO and by Amrhein and Suarez (1988) for anorthite. One glass, SLN, has measured dissolution rates that are inconsistent with this surface coordination model. Its inconsistent behaviour may be related to iron coatings that were detected on its surface (SEM images not shown). These weathering features could have influenced the surface complexation. Nevertheless, the linear trends illustrated in Figure 8 demonstrate that the surface coordination model is consistent with the glass dissolution rate data obtained in this study. As such it is not possible to distinguish unambiguously between the surface coordination and the multi-oxide dissolution mechanisms from the data measured in the present study.

Despite the consistency between the surface coordination model and measured rates for four of the glasses considered in the present study, it is not possible to generate a single equation describing the rates of natural glass dissolution rates as a function of their composition using this model for several
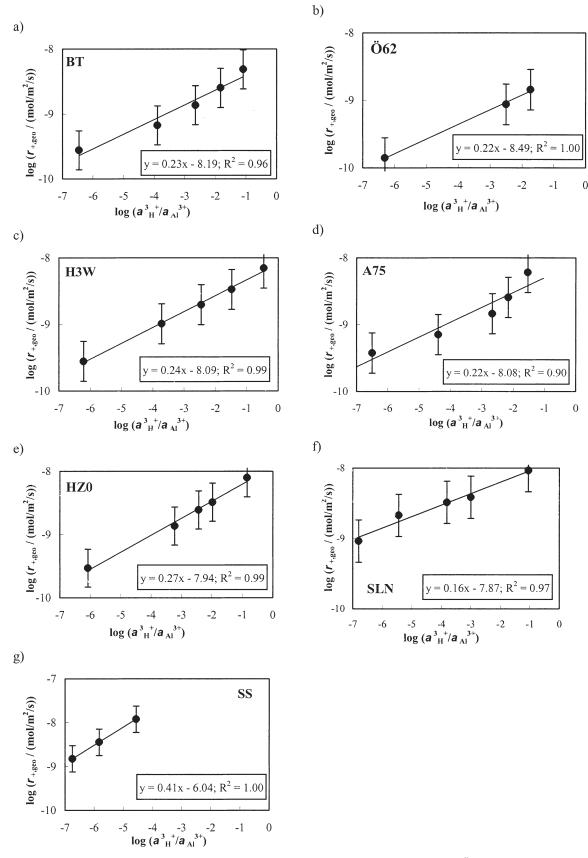
Fig. 4. The logarithmic far-from-equilibrium dissolution rates, log $r_{+,geo}$ of a) BT (rhyolite), b) Ö62 (ryholite), c) H3W (rhyolite), d) A75 (rhyolite), e) HZ0 (dacite), f) SLN (dacite), g) SS (basalt) as a function of log $(a^3_{H+}/a_{Al^{3+}})$. The symbols represent measured rates but the lines correspond to a linear least squares fit of these data. The equation and correlation coefficient (R^2) of each fit is provided in the figure. The slope denotes the stoichiometric coefficient n and the y-intercept stands for the logarithmic rate constant k (see text).
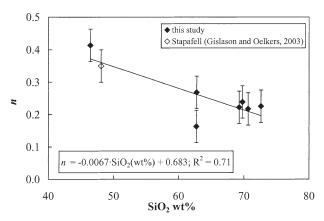
Fig. 5. The stoichiometric coefficient n (Eqn. 1 and 2) as a function of the silica content of the glasses. The symbols correspond to n values generated from the slopes of the fits illustrated in Figure 4. The line through the data represents a linear least square fit of n from the values of this study; the equation and correlation coefficient (R^2) of this fit are provided. The error bars correspond to an estimated ± 0.05 uncertainty in n.

reasons. First, the relatively small number of data points measured from each glass over a relatively small range of total aqueous fluoride concentrations, spanning less than one order of magnitude, results in significant scatter among the k_L and l values obtained from regression calculations. Moreover, the surface coordination model requires additional parameters to describe the effects on dissolution rates of each present aqueous component, and thus require far more data to quantify rates for each glass composition. Such is not the case of the Oelkers (2001) multi-oxide dissolution model, which has successfully described the dissolution rates of basaltic glass over extensive pH ranges in the presence of a variety of aqueous components using a single value of n and k (cf. Oelkers and Gislason, 2001).
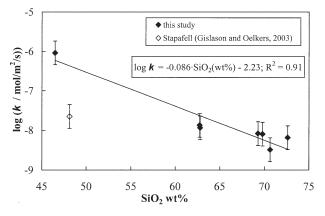

Fig. 6. The logarithm of the rate constant k (Eqn. 1 and 2) as a function of the silica content of the glasses. The symbols correspond to measured rate constants obtained from the intercepts of the fits illustrated in Figure 4. The line through the data represents a linear least squares fit from the values of this study; the equation and correlation coefficient (R^2) of this fit are provided. The error bars correspond to an estimated ± 0.3 log unit uncertainty in these rate constants.
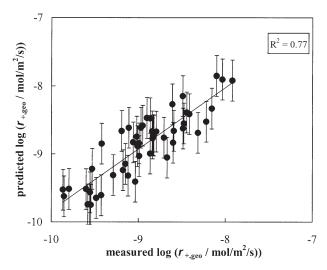

Fig. 7. Comparison between predicted and measured far-from-equilibrium forward dissolution rates $r_{+,geo}$ at pH 4 and 25°C using Eqn. (8). The symbols in this figure correspond to both rates reported in the present study and those reported by Wolff-Boenisch et al. (2004). The line in this figure corresponds to equal values for these rates; the error bars correspond to an estimated ± 0.3 log unit uncertainty in these rates.

4.3. Fluoride Dissolution Rate Enhancement in Natural Environments

Eqn. 8 allows prediction of surface-reaction controlled, far-from-equilibrium natural glass dissolution rates as a function of both glass and aqueous solution composition at 25°C. One example of such a calculation is illustrated in Figure 9 for the rhyolitic glass BT. The curves in this figure were all generated using aqueous activities computed with PRHEEQC 2.6 at a total Al concentration of 10^{-6} mol/kg and the fluoride concentrations given in the legend. Note that all aqueous species present in solution have the potential to alter glass dissolution rates. For example, the presence of aqueous Si can provoke the formation of aqueous Si-F complexes, which would lower the quantity of F^- available to form aqueous Al-F complexes. The bold dashed line in Figure 9 represents $r_{+,geo}$ as a function of pH in the absence of aqueous fluoride. The other four curves illustrate how $r_{+,geo}$ varies with increasing F concentration. Glass dissolution rates are strongly affected by the presence of aqueous fluoride at acid to neutral conditions. In contrast, there is no predicted dissolution promoting effect of aqueous F at pH > 7.5; this stems from the lack of aqueous Al-fluoride complexing at these conditions. The significance of fluoride glass dissolution rate enhancement at acid pH can be illustrated by comparing the fluoride effect on rates with that of temperature. For example, the presence of 90 μmol of total aqueous F (≈ 1.7 ppm) increases $r_{+,geo}$ of rhyolitic glass dissolution rates by approximately the same amount as a temperature increase from 25°C to ~75°C (Wolff-Boenisch et al., 2004).

The degree to which aqueous fluoride rate enhancement of aluminosilicate glasses and minerals is significant in natural processes depends on the system. There are a number of sources of aqueous fluoride in volcanic environments. Rapid losses of F from fresh volcanic deposits were reported during leaching by rain resulting in F concentrations up to 8
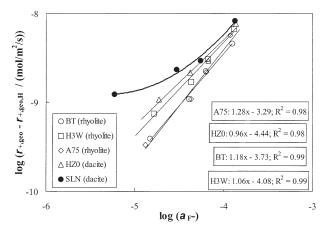
Fig. 8. The logarithm of the difference between the dissolution rate ($r_{+,geo}$) and the dissolution rate without a ligand-promoting effect ($r_{+,geo,H}$) versus the logarithm of the fluoride activity. The symbols correspond to measured rates of the glasses BT, H3W A75, and HZ0 and the linear curves through the symbols represent a linear least squares fit of these data sets. The equation and correlation coefficient (R^2) of these fits are provided in the figure. The data for the glass SLN are inconsistent with a linear fit and have been traced using a bold curve.

ppm in streams in the regions of ash fall (Stefánsson and Sigurjónsson, 1957; Óskarsson, 1980; Gíslason et al., 1992). Ellis and Mahon (1963, 1967) also suggested that significant F in rhyolite glass occurs as surficial coatings and Óskarsson (1980) and Frogner et al. (2001) found that F is chemically adsorbed on the surface of andesitic tephra particles in the cooling eruption column and is rapidly released as pristine tephra comes in contact with surface waters. White and Hochella (1992) ascribed the enrichment of F on the surfaces of unweathered glassy rinds of chilled tholeiitic lava flows to the formation of water-soluble salts like CaF_2, MgF_2, and AlF_3. Moreover, rainwater in volcanic regions itself contains fluoride. Symonds et al. (1988), Thordarson et al. (1996), and Thordarson and Self (1996) reported that large volcanic eruptions may inject significant amounts of HF into the stratosphere and that passively degassing volcanoes are also a major source of tropospheric HF. In places like the East African Rift Valley the principal source of fluoride relates to emissions from volcanic activity, which can release abundant F into waters to be further concentrated by strong evapotranspiration to reach levels up to 10–20 ppm in potable water (Gaciri and Davis, 1993; Reimann et al., 2003). A paradigm case is subglacial eruptions and snow-ash interactions, where volatile components including HF or SiF_4 are condensed immediately and fluoride concentrations can therefore build up in the meltwater reaching 1200 ppm (Gislason et al., 1992; 2002). Symonds et al. (1988) showed that HCl and HF are the dominant species of Cl and F in volcanic gases, at least several orders of magnitude more abundant than all other Cl and F species. The pH of these meltwaters ranges from 2 to 7 so that ideal conditions prevail for the dissolution of tephra glass particles as shown in Figure 9. The observations summarized above suggest that aqueous fluoride concentrations are sufficient in many volcanic systems to increase natural glass dissolution rates by an order of magnitude or more.

Aqueous fluoride is also found in abundance in other natural environments. Lahermo et al. (1991) reported high F concentration anomalies in soils, natural surface waters and shallow groundwaters as a result of draining high F (Rapakivi) granites in Finland. Other high groundwater fluoride concentrations associated with igneous and metamorphic rocks have been reported from India, West Africa, Thailand, China, and Southern Africa. Geothermal fluids are also commonly noted to be rich in aqueous fluoride. For example, the natural thermal waters of New Zealand were found to have fluoride concentrations ranging from 1 to 12 ppm (Mahon, 1964), hot springs and geysers of Yellowstone National Park were reported to have aqueous fluoride concentrations from 25–50 ppm (Neuhold and Sigler, 1962) and Icelandic geothermal waters vary from 0.1 to 19 ppm (Arnorsson et al., 1983). According to Murrmann and Koutz (1972) the concentration of F in soil solutions commonly ranges from 0.1–0.5 ppm. The latter value is close to the lowest F concentration of this study (30 μM, see Fig. 3), so the dissolution rate enhancing effect of fluoride may be as significant as that of organic acids. Other favourable environments of high aqueous fluoride concentrations and low pH are anthropogenic, e.g., drainage waters from watersheds that are affected by acid rain. This is especially the case where the manufacture of phosphoric acid and phosphate fertilizers occurs (Van Craenenbroeck and Marivoet, 1987). Other potential F contamination sources include the fluoridation of drinking water supplies, the application of F-containing fertilizers and pesticides, and heavy industries, such as steel, glass, cement, aluminium smelters and power stations (Leece and Scheltema, 1983; Fuge and Andrews, 1988; Skjelkvåle, 1994; Camargo, 1996; Roy et al., 2000).
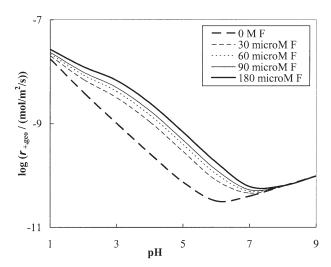

Fig. 9. The logarithm of $r_{+,geo}$ versus the pH for the rhyolitic glass BT. The curves were all calculated using Eqn. 8. The aqueous activities were computed with PRHEEQC 2.6 at a total Al concentration of 10^{-6} mol/kg and the fluoride concentrations given in the legend. The bold dashed line represents $r_{+,geo}$ as a function of pH in the absence of aqueous fluoride. The other four lines display how $r_{+,geo}$ increases with increasing F concentration.

5. CONCLUSIONS

This study demonstrates that the presence of aqueous fluoride in acid solutions increases significantly natural glass dissolution rates. This dissolution promoting effect can be accounted for using the surface coordination model of Stumm (1992) or the multi-oxide dissolution model of Oelkers (2001). Application of the latter model yields a rate expression that can be used to predict far-from-equilibrium dissolution rates as a function of both glass and aqueous solution composition. It is thus a powerful tool for estimating natural glass dissolution rates in a variety of natural environments. Consideration of the compositions of natural solutions suggests that the presence of aqueous fluoride can increase natural glass dissolution rates by an order of magnitude or more. In such systems the degree of fluoride rate enhancement may be of organic acid anions.

REFERENCES

Allnatt A. R., Bancroft G. M., Fyfe W. S., Jacobs P. W. M., Karkhanis S. N., Melling P. J., Nishijima A., Vempati C. S., and Tait J. (1983) Leaching behaviour and electrical conductivity of natural rhyolite and modified synthetic rhyolites. *Chem. Geol.* **38,** 329–357.

Amrhein C. and Suarez D. L. (1988) The use of surface complexation model to describe the kinetics of ligand-promoted dissolution of anorthite. *Geochim. Cosmochim. Acta* **52,** 2785–2793.

Anbeek C. (1992a) Surface roughness for minerals and implications for dissolution studies. *Geochim. Cosmochim. Acta* **56,** 1461–1469.

Anbeek C. (1992b) The dependence of dissolution rates on grain size for some fresh and weathered feldspars. *Geochim. Cosmochim. Acta* **56,** 3957–3970.

Anbeek C. (1993) The effect of natural weathering on dissolution rates. *Geochim. Cosmochim. Acta* **57,** 4963–4975.

Arnalds Ó. and Kimble J. (2001) Andisols of deserts in Iceland. *Soil Sci. Soc.* **65,** 1778–1786.

Arocena J. M., Dudas M. J., Poulsen L., and Rutherford P. M. (1995) Weathering of clay minerals induced by fluoride-containing solutions from phosphogypsum by-product. *Can. J. Soil Sci.* **75,** 219–226.

Bacon F. R. and Raggon F. C. (1959) Promotion of attack on glass and silica by citrate and other anions in neutral solution. *J. Am. Ceram. Soc.* **42,** 199–205.

Berger G., Schott J., and Loubet M. (1987) Fundamental processes controlling the first stage of alteration of a basaltic glass by seawater: An experimental study between 200 and 320°C. *Earth Planet. Sci. Lett.* **84,** 431–445.

Brady P. V. and Carroll S. A. (1994) Direct effects of CO₂ and temperature on silicate weathering: Possible implications for climate control. *Geochim. Cosmochim. Acta* **58,** 1853–1856.

Brantley S. L. and Chen Y. (1995) Chemical weathering rates of pyroxenes and amphibols. In *Chemical weathering rates of silicate minerals* (eds. A. F. White and S. L. Brantley), *Rev. Mineral.* **31,** 119–172.

Brantley S. L., White A. F., and Hodson M. (1999) Surface area of primary silicate minerals. In *Growth, dissolution and pattern formation in geosystems* (eds. B. Jamtveit and P. Meakin), pp. 291–326. Kluwer Academic Publishers USA.

Camargo J. A. (1996) Comparing levels of pollutants in regulated rivers with safe concentrations of pollutants for fishes: A case study. *Chemosphere* **33,** 81–90.

Chadwick O. A., Gavenda R. T., Kelly E. F., Ziegler K., Olson C. G., Elliott W. C., and Hendricks D. M. (2003) The impact of climate on the biogeochemical functioning of volcanic soils. *Chem. Geol.* **202,** 195–223.

Crovisier J. L., Honnorez J., and Eberhart J. P. (1987) Dissolution of basaltic glass in seawater: Mechanism and rate. *Geochim. Cosmochim. Acta* **51,** 2977–2990.

Dahlgren R., Shoji S., and Nanzyo M. (1993) Mineralogical characteristics of volcanic ash soils. In *Volcanic ash soils. Genesis, Properties, and Utilization* (eds. S. Shoji, M. Nanzyo and R. Dahlgren), pp. 101–143. Elsevier, Amsterdam.

Drever J. I. and Stillings L. L. (1997) The role of organic acids in mineral weathering. *Coll. Surf. A: Physicochem. Eng. Aspects.* **120,** 167–181.

Driscoll C. T., Baker J. P., Bisogni J. J., and Schofield C. L. (1980) Effect of aluminium speciation on fish in dilute acidified waters. *Nature* **284,** 161–164.

Dubroeucq D., Geissert D., and Quantin P. (1998) Weathering and soil forming processes under semi-arid conditions in two Mexican volcanic ash soils. *Geoderma* **86,** 99–122.

Ellis A. J. and Mahon W. A. J. (1963) Natural hydrothermal systems and experimental hot water-rock interactions. *Geochim. Cosmochim. Acta* **28,** 1323–1357.

Ellis A. J. and Mahon W. A. J. (1967) Natural hydrothermal systems and experimental hot water-rock interactions (Part II). *Geochim. Cosmochim. Acta* **31,** 519–538.

Elrashidi M. A. and Lindsay W. L. (1987) Effect of fluoride on pH, organic matter and solubility of elements in soils. *Environ. Pollut.* **47,** 123–133.

Ernsberger F. M. (1959) Attack of glass by chelating agents. *J. Am. Ceram. Soc.* **42,** 373–375.

Fiore S., Huertas F. J., Tazaki K., Huertas F., and Linares J. (1999) A low temperature experimental alteration of a rhyolitic obsidian. *Eur. J. Mineral.* **11,** 455–469.

Frogner P., Gíslason S. R., and Óskarsson N. (2001) Fertilizing potential of volcanic ash in ocean surface water. *Geology* **29,** 487–490.

Fuge R. and Andrews M. J. (1988) Fluorine in the UK environment. *Environ. Geochem. Health* **10,** 96–104.

Furrer G. and Stumm W. (1986) The coordination chemistry of weathering: I. Dissolution kinetics of δ-Al₂O₃ and BeO *Geochim. Cosmochim. Acta* **50,** 1847–1860.

Gaciri S. J. and Davis T. C. (1993) The occurrence and geochemistry of fluoride in some natural waters of Kenya. *J. Hydrol.* **143,** 395–412.

Gajam S. Y. and Raghavan S. (1985) A kinetic model for the hydrochloric acid leaching of kaolinite clay in the presence of fluoride ions. *Hydrometall.* **15,** 143–158.

Gautier J.-M., Oelkers E. H., and Schott J. (2001) Are quartz dissolution rates proportional to BET surface areas? *Geochim. Cosmochim. Acta* **65,** 1059–1070.

Gislason S. R. and Oelkers E. H. (2003) The mechanism, rates, and consequences of basaltic glass dissolution: II. An experimental study of the dissolution rates of basaltic glass as a function of pH at temperatures from 6°C to 150°C. *Geochim. Cosmochim. Acta* **67,** 3817–3832.

Gislason S. R., Andrésdóttir A., Sveinbjörnsdóttir Á. E., Óskarsson N., Thordarson Th., Torsander P., Novâk M., and Zâk K. (1992) Local effects of volcanoes on the hydrosphere: Example from Hekla, southern Iceland. In *Water-Rock Interactions* (eds. Y. K. Kharaka and A. S. Maest), pp. 477–481. Balkema, Rotterdam.

Gislason S. R., Arnórsson S., and Ármannsson H. (1996) Chemical weathering of basalt in SW Iceland: Effects of runoff, age of rocks and vegetative/glacial cover. *Am. J. Sci.* **296,** 837–907.

Gislason S. R., Snorrason Á., Kristmannsdóttir H. K., Sveinbjörnsdóttir Á. E., Torsander P., Ólafsson J., Castet S., and Dupré B. (2002) Effects of volcanic eruptions on the CO₂ content of the atmosphere and the oceans: The 1996 eruption and flood within the Vatnajökull Glacier, Iceland. *Chem. Geol.* **190,** 181–205.

Grambow B. (1985) A general rate equation for nuclear waste glass corrosion. *Mat. Res. Soc. Symp. Proc.* **44,** 15–27.

Grandstaff D. E. (1977) Some kinetics of bronzite orthopyroxene dissolution. *Geochim. Cosmochim. Acta* **41,** 1097–1103.

Guy C. and Schott J. (1989) Multisite surface reaction versus transport control during hydrolysis of a complex oxide. *Chem. Geol.* **78,** 181–204.

Harouiya N. and Oelkers E. H. (2004) An experimental study of the effect of aqueous fluoride on quartz and alkali-feldspar dissolution rates. *Chem. Geol.*, **205,** 155–167.

Huang P. M. and Jackson M. L. (1965) Mechanism of reaction of neutral fluoride solution with layer silicates and oxides of soils. *Soil Sci. Soc. Proc.* **29,** 661–665.

Huang W. H. and Kiang W. C. (1972) Laboratory dissolution of plagioclase feldspars in water and organic acids at room temperature. *Am. Mineral.* **57,** 1849–1859.

Jaycock M. J. and Parfitt G. D. (1981) Chemistry of interfaces. E. Horwood, Chichester.

Kraemer S. M., Chiu V. Q., and Hering J. G. (1998) Influence of pH and competitive adsorption on the kinetics of ligand-promoted dissolution of aluminium oxide. *Environ. Sci. Technol.* **32,** 2876–2882.

Lahermo P., Sandström H., and Malisa E. (1991) The occurrence and geochemistry of fluorides in natural waters in Finland and East Africa with reference to their geomedical implications. *J. Geochem. Explor.* **41,** 65–79.

Leece D. R. and Scheltema J. H. (1983) Effects of fluoride emissions from industry on the fluoride concentration of grape leaves (Vitis vinifera) in New South Wales. In *Fluorides—effects on vegetation, animals and humans* (eds. J. L. Shupe, H. B. Peterson and N. C. Leone), pp. 127–134. Paragon Press, Salt Lake City, Utah.

Luther S. M., Poulsen L., Dudas M. J., and Rutherford P. M. (1996) Fluoride sorption and mineral stability in an Alberta soil interacting with phosphogypsum leachate. *Can. J. Soil Sci.* **76,** 83–91.

Mahon W. A. J. (1964) Fluorine in natural thermal waters of New Zealand. *New Zealand J. Sci.* **7,** 3–28.

Moulton K. L., West J., and Berner R A. (2000) Solute flux and mineral mass balance approaches to the quantification of plant effects on silicate weathering. *Am. J. Sci.* **300,** 539–570.

Murphy W. M., Oelkers E. H., and Lichtner P. C. (1989) Surface reaction versus diffusion control of mineral dissolution and growth rates in geochemical processes. *Chem. Geol.* **78,** 357–380.

Murrmann R. P. and Koutz F. R. (1972) Role of soil chemical processes in reclamation of wastewater applied to land. In *Wastewater management by disposal on the land* (ed. S. C. Reed), Special Report 171, pp. 48–76. US Army Cold Regions Research and Engineering Laboratory, Hanover, New Hampshire.

Neuhold J. M. and Sigler W. F. (1962) Chlorides affect the toxicity of fluoride in rainbow trout. *Science* **135,** 732–733.

Nieuwenhuyse A., Verburg P. S. J., and Jongmans A. G. (2000) Mineralogy of a soil chronosequence on andesitic lava in humid tropical Costa Rica. *Geoderma* **98,** 61–82.

Nordin J. P., Sullivan D. J., Phillips B. L., and Casey W. H. (1998) An ^{17}O-NMR study of the exchange of water on $AlOH(H_2O)_5^{2+}$ (aq). *Inorg. Chem.* **37,** 4760–4763.

Nordin J. P., Sullivan D. J., Phillips B. L., and Casey W. H. (1999) Mechanisms for fluoride-promoted dissolution of bayerite [β-Al(OH)$_3$(s)] and boehmite [γ-AlOOH]: ^{19}F-NMR spectroscopy and aqueous surface chemistry. *Geochim. Cosmochim. Acta* **63,** 3513–3524.

Oelkers E. H. (2001) A general kinetic description of multi-oxide silicate mineral and glass dissolution. *Geochim. Cosmochim. Acta* **65,** 3703–3719.

Oelkers E. H. and Gislason S. R. (2001) The mechanism, rates, and consequences of basaltic glass dissolution: I. An experimental study of the dissolution rates of basaltic glass as a function of aqueous Al, Si, and oxalic acid concentration at 25°C and pH = 3 and 11. *Geochim. Cosmochim. Acta* **65,** 3671–3681.

Oelkers E. H., Schott J., and Devidal J.-L. (1994) The effect of aluminium, pH, and chemical affinity on the rates of aluminosilicate dissolution reactions. *Geochim. Cosmochim. Acta* **58,** 2011–2024.

Óskarsson N. (1980) The interaction between volcanic gases and tephra: Fluorine adhering to tephra of the 1970 Hekla eruption. *J. Volcanol. Geotherm. Res.* **8,** 251–266.

Parkhurst D. L. and Appelo C. A. J. (1999) User's guide to PHREEQC (Version 2)—A computer program for speciation, batch-reaction, one-dimensional transport, and inverse geochemical calculations. *U. S. G. S. Water Resour. Inv. Report.* 99–4259.

Petit J.-C., Della Mea G., Dran J.-C., Magonthier M.-C., Mando P. A., and Paccagnella A. (1990) Hydrated-layer formation during dissolution of complex silicate glasses and minerals. *Geochim. Cosmochim. Acta* **54,** 1941–1955.

Plankey B. J., Patterson H. H., and Cronan C. S. (1986) Kinetics of aluminium fluoride complexation in acidic waters. *Environ. Sci. Technol.* **20,** 160–165.

Reimann C., Bjorvatn K., Frengstad B., Melaku Z., Tekle-Haimanot R., and Siewers U. (2003) Drinking water quality in the Ethiopian section of the East African Rift Valley I—data and health aspects. *Sci. Total Environ.* **311,** 65–80.

Roy R. L., Campbell P. G. C., Prémont S., and Labrie J. (2000) Geochemistry and toxicity of aluminium in the Saguenay River, Quebec, Canada, in relation to discharges from an aluminium smelter. *Environ. Toxicol. Chem.* **19,** 2457–2466.

Shoji S., Nanzyo M., Shirato Y., and Ito T. (1993) Chemical kinetics of weathering in young andisols from northeastern Japan using soil age normalized to 10°C. *Soil Sci.* **155,** 53–60.

Shotyk W. and Nesbitt H. W. (1992) Incongruent and congruent dissolution of plagioclase feldspar: effect of feldspar composition and ligand complexation. *Geoderma* **55,** 55–78.

Skjelkvåle B. L. (1994) Water chemistry in areas with high deposition of fluoride. *Sci. Total Environ.* **152,** 105–112.

Steel K. M., Besida J., O'Donnell T. A., and Wood D. G. (2001) Production of ultra clean coal. Part I—Dissolution behaviour of mineral matter in black coal toward hydrochloric and hydrofluoric acids. *Fuel Process. Technol.* **70,** 171–192.

Stefánsson K. and Sigurjónsson J. (1957) Temporary increase in fluorine content of water following the eruption: The eruption of Hekla, 1947–1948. *Soc. Sci. Islandia* **III,** 1–13.

Stefánsson A. and Gíslason S. R. (2001) Chemical weathering of basalts, SW Iceland: Effect of rock crystallinity and secondary minerals on chemical fluxes to the ocean. *Am. J. Sci.* **301,** 513–556.

Stumm W. (1992) Chemistry of the solid-water interface. J. Wiley & Sons, New York.

Stumm W. (1997) Reactivity at the mineral-water interface: dissolution and inhibition. *Colloids Surf. A: Physicochem. Eng. Aspects.* **120,** 143–166.

Supriyo H., Matsue N., and Yoshinaga N. (1992) Chemical and mineralogical properties of volcanic ash soils from Java. *Soil Sci. Plant Nutr.* **38,** 443–457.

Symonds R. B., Rose W. I., and Reed M. H. (1988) Contribution of Cl- and F- bearing gases to the atmosphere by volcanoes. *Nature* **334,** 415–418.

Tagirov B. and Schott J. (2001) Aluminum speciation in crustal fluids revisited. *Geochim. Cosmochim. Acta* **65,** 3965–3992.

Tagirov B., Schott J., and Harrichoury J.-C. (2002) Experimental study of aluminum-fluoride complexation in near neutral and alkaline solutions to 300°C. *Chem. Geol.* **184,** 301–310.

Taniguchi H. (1980) Some volcano-geological significances of the hydration layer observed in the glassy groundmass of Kozu-shima rhyolite. *Bull. Volcanol. Soc. Jpn.* **25,** 217–229.

Tester J. W., Worley W. G., Robinson B. A., Grigsby C. O., and Feerer J. L. (1994) Correlating dissolution kinetics in pure water from 25° to 625°C. *Geochim. Cosmochim. Acta* **58,** 2407–2420.

Thordarson T. and Self S. (1996) Sulfur, chlorine, and fluorine degassing and atmospheric loading by the Roza eruption, Columbia River Basalt Group, Washington, USA. *J. Volcanol. Geotherm. Res.* **74,** 49–73.

Thordarson T., Self S., Óskarsson N., and Hulsebosch T. (1996) Sulfur, chlorine, and fluorine degassing and atmospheric loading by the 1783–1784 AD Laki eruption in Iceland. *Bull. Volcanol.* **58,** 205–225.

Ullman W. J. and Welch S. A. (2002) Organic ligands and feldspar dissolution. In *Water-rock Interactions, Ore Deposits, and Environmental Geochemistry: A tribute to David A. Crerar* (eds. R.

Hellmann and S. A. Woods), vol. 7, 3–35. Geochemical Society, Special Publication Series USA.

Vacca A., Adamo P., Pigna M., and Violante P. (2003) Genesis of tephra-derived soils from the Roccamonfina volcano, south central Italy. *Soil Sci. Soc.* **67,** 198–207.

Van Craenenbroeck W. and Marivoet J. (1987) A comparison of simple methods for estimating the mass flow of fluoride discharged into rivers. *Water Sci. Tech.* **19,** 729–740.

White A. F. (1983) Surface chemistry and dissolution kinetics of glassy rocks at 25°C. *Geochim. Cosmochim. Acta* **47,** 805–815.

White A. F. and Claassen H. C. (1980) Kinetic model for the short-term dissolution of a rhyolitic glass. *Chem. Geol.* **28,** 91–109.

White A. F. and Hochella M. F. Jr. (1992) Surface chemistry associated with the cooling and subaerial weathering of recent basalt flows. *Geochim. Cosmochim. Acta* **56,** 3711–3721.

Wieland E., Wehrli B., and Stumm W. (1988) The coordination chemistry of weathering: III. A generalization on the dissolution rates of minerals *Geochim. Cosmochim. Acta* **52,** 1969–1981.

Wolff-Boenisch D., Gislason S. R., Oelkers E. H., and Putnis C. V. (2004) The dissolution rates of natural glasses as a function of their composition at pH 4 and 10.6, and temperatures from 25 to 74°C. *Geochim. Cosmochim. Acta*, in press.

Zŭtić V. and Stumm W. (1984) Effect of organic acids and fluoride on the dissolution kinetics of hydrous alumina. A model study using the rotating disc electrode. *Geochim. Cosmochim. Acta* **48,** 1493–1503.